ELSEVIER

Journal of Alloys and Compounds 434–435 (2007) 225–228

Journal of ALLOYS AND COMPOUNDS

www.elsevier.com/locate/jallcom

# High temperature oxidation of the refractory alloy glass $Nb_{35}Ni_{60}Sn_5$

Isabella Gallino [a,*], Ralf Busch [a,1], Haein Choi Yim [b], Lioba Jastrow [c], Uwe Köster [c]

[a] *Department of Mechanical Engineering, Oregon State University, Corvallis, OR 97331, USA*
[b] *W. M. Keck Laboratory of Engineering Materials, California Institute of Technology, Pasadena, CA 91125, USA*
[c] *Department of Biochemical & Chemical Engineering, University of Dortmund, D-44221 Dortmund, Germany*

Available online 17 October 2006

**Abstract**

The newly discovered Ni–Nb–Sn glass is considered a promising refractory material due to its high glass transition temperature ($T_g > 880$ K). An adequate oxidation resistance at high temperatures is therefore necessary. In this paper the oxidation behavior of the $Nb_{35}Ni_{60}Sn_5$ refractory alloy glass has been studied in dry air in the temperature range of about 803–863 K. Isothermal thermogravimetric analyses reveal paralinear oxidation kinetics with similar oxidation rates that Zr-based glasses experience 200 K below these temperatures. X-ray diffraction and cross-sectional electron microscopy allows phase identification in the scales revealing their formation mechanism. The oxide scale resulting from oxidation consists of an outer layer of Ni oxide and a continuous inner layer of Nb oxide. This sequence of different oxide layers is repeated as the oxidation proceeds. The depletion of Nb in the alloy underneath the scale seems to induce the crystallization of Ni-rich intermetallics such as $NbNi_3$ and the ternary intermetallic $NbNi_2Sn$. Thermodynamics and kinetic aspects of the interaction between oxidation and crystallization are also discussed.


*Keywords:* Amorphous materials; Calorimetry; Oxidation; Scanning electron microscopy; SEM; X-ray diffraction

## 1. Introduction

Refractory Ni-based bulk metallic glasses with extremely high glass forming ability (GFA) and excellent stability with respect to crystallization have been recently discovered within the simple ternary system Nb–Ni–Sn [1]. The composition of these refractory alloy glasses (RAG) has been found by tailoring the composition near the ternary eutectic composition located within the three-phase region defined by the three intermetallics $NbNi_3$, $Nb_7Ni_6$ (μ-phase), and $NbNi_2Sn$ ($BiF_3$-type). These alloys show exceptionally high Vickers hardness (1000–1280 VH), strength (3–3.8 GPa), elastic modulus (180–200 GPa), along with very high values of the glass transition temperature $T_g$ (881–895 K) [1]. These mechanical and thermal properties exceed those of previously reported Ni-based bulk amorphous alloys [3–5], making this RAG system a promising refractory material. This paper reports upon the first investigation on high temperature air oxidation (803–863 K) of the RAG $Nb_{35}Ni_{60}Sn_5$. The results are discussed in terms of thermodynamics and kinetics including that for the interaction between oxidation and crystallization.

## 2. Experimental procedures

Glassy 1 mm-thick strips of $Nb_{35}Ni_{60}Sn_5$ were prepared by re-melting previously arc-melted master alloys in an evacuated quartz tube with a radiofrequency induction coil and subsequent injection cast into a copper mold as described in Ref. [1]. Specimens of regular shape were cut with a slow diamond saw and polished up to 1200 grid. The surface area was measured and was in the order of 1 $cm^2$. These glassy specimens were analyzed in isothermal thermogravimetry with 30 ml/min of synthetic air at temperatures below the calorimetric glass transition, $T_g$. DSC and DTA calorimetric measurements as well as vacuum isothermal treatments in a quartz tube furnace under a $10^{-6}$ mbar atmosphere were performed to study the thermal stability of the glass with respect to crystallization. The microstructure was characterized by X-ray diffraction analyses (with Cu Kα radiation) as well as scanning and transmission electron microscopy (SEM and TEM).

## 3. Results and discussion

The refractory alloy glass $Nb_{35}Ni_{60}Sn_5$ shows excellent stability with respect to crystallization, which is reflected by its high glass transition temperature, 200 K higher than the known

* Corresponding author. Permanent and present address: University of Saarland, Department of Materials Science, D-66041 Saarbrücken, Germany. Tel.: +1 49 681 3022052; fax: +1 49 681 3024385.
*E-mail address:* i.gallino@mx.uni-saarland.de (I. Gallino).
[1] Permanent and present address: University of Saarland, Department of Materials Science, Chair for Metallic Materials, D-66041 Saarbrücken, Germany.

0925-8388/$ – see front matter © 2006 Elsevier B.V. All rights reserved.
doi:10.1016/j.jallcom.2006.08.101

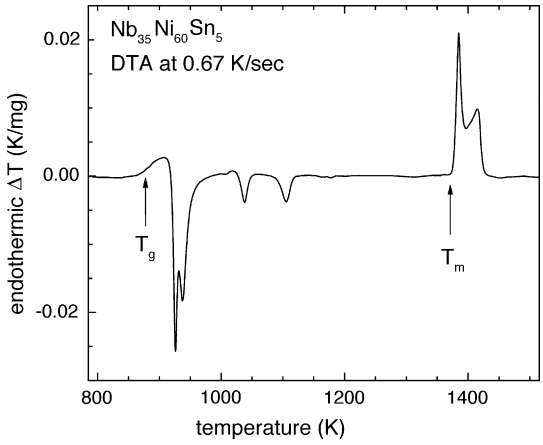


Fig. 1. DTA thermogram of the as-cast $Nb_{35}Ni_{60}Sn_5$ alloy at a constant heating rate of 0.167 K/s.

Zr-based glasses. Fig. 1 is a differential thermal (DTA) thermogram of an as-cast sample scanned with a heating rate of 0.167 K/s. The $T_g$, defined as the onset of the calorimetric glass transition, occurs at about 883 K. The temperatures for the isothermal oxidation study have been selected 20–60 K below $T_g$. During heating the supercooled liquid crystallizes between $T_g$ and the eutectic temperature, $T_m$ (1373 K) with a total of four exothermic events.

Fig. 2 shows the lower half of the time temperature transformation (TTT) diagram for $Nb_{35}Ni_{60}Sn_5$ constructed from isothermal calorimetric (DSC) crystallization experiments. The crystallization occurs *via* two consecutive exothermic reactions. The isothermal calorimetric glass transition is calculated from the $T_g$ shift at various heating rates and indicates the relaxation time at each temperature [6]. The oxidation times have been selected, on average, 25% shorter than the time for the onset of crystallization.

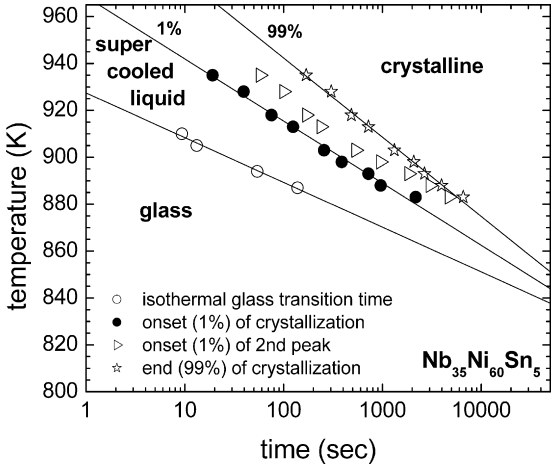


Fig. 2. Lower half of the time temperature transformation (TTT) diagram constructed from isothermal calorimetric crystallization experiments. The onset (1%) and the end (99%) of the crystallization event are plotted in full circles and start symbols, respectively. The crystallization occurs in two exothermic reactions and the onset of the second peak is shown as triangles. The calorimetric glass transition is calculated from the $T_g$ shift at various heating rates taken from [3].

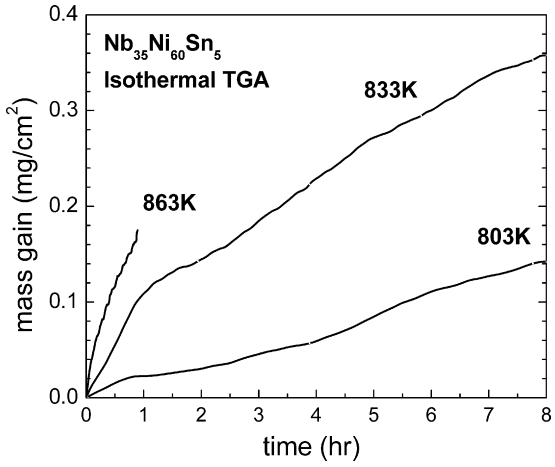


Fig. 3. TGA kinetics curves for the oxidation of the as-cast $Nb_{35}Ni_{60}Sn_5$ at 803, 833, and 863 K.

Fig. 3 reports the thermogravimetric (TGA) curves for the isothermal oxidation of the as-cast alloys at 803, 833, and 863 K. The oxidation rates are similar to the rates that Zr-based glasses experience already at temperatures of 600–650 K [2]. The curves show paralinear oxidation indicating a kinetic of growth of multilayered scales where an inner compact oxide grows diffusion-controlled, and the outside scale breaks down.

Fig. 4 shows a SEM micro-photograph of the cross-section of the RAG $Nb_{35}Ni_{60}Sn_5$ oxidized for 8 h at 833 K. The oxide scale appears to be compact and continuous. Discontinuities crystal-like appear growing internally towards the matrix alloy. The matrix appears depleted underneath the scale. Preliminary cross-sectional TEM analysis revealed a fully crystallized matrix after 80 h of air oxidation at 803 K. This isothermal crystallization was not expected according to the TTT diagram of Fig. 2. In Fig. 5 two types of crystals of the order of 100 nm are marked.

Fig. 6 shows the X-ray diffractograms of the as-cast alloy and after selected annealing. The broad peak characteristic of amorphous materials is seen in the as-cast (1) as well as after

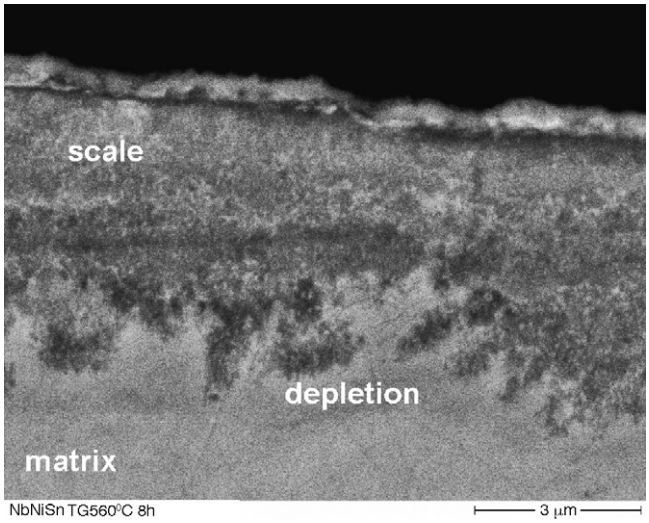


Fig. 4. SEM micro-photograph of the cross-section of the RAG $Nb_{35}Ni_{60}Sn_5$ oxidized for 8 h at 833 K.

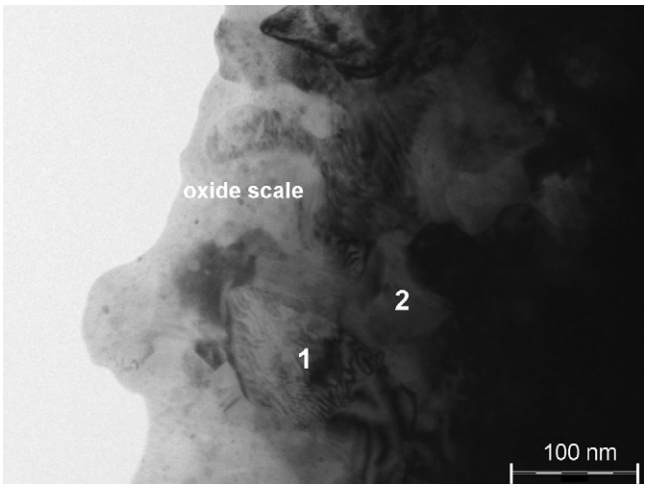


Fig. 5. Cross-sectional TEM photomicrograph of the RAG $Nb_{35}Ni_{60}Sn_5$ oxidized for 80 h at 803 K. The oxide scale as well as two types of crystals of the order of 100 nm are visible. The matrix appears fully crystallized.

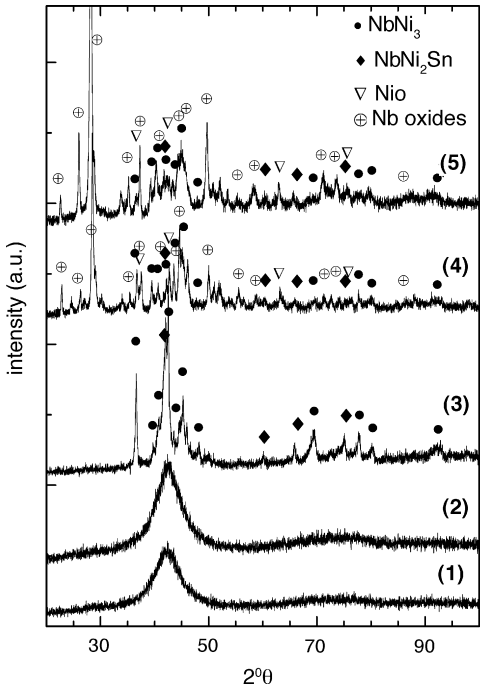


Fig. 6. X-ray diffractograms of the as-cast alloy (1) and after selected vacuum annealing at 853 K for 8 h (2) and at 883 K for 2 h (3), and after isothermal air oxidation at 803 K for 80 h (4) and at 833 K for 8 h (5).

vacuum annealing at 853 K for 8 h (2). The crystallization of Ni-rich intermetallics such as $NbNi_3$ and $NbNi_2Sn$ occurs during 2 h of isothermal vacuum annealing at 883 K (3). These intermetallics are found in samples oxidized at 833 K for 8 h (5) and at lower temperatures, e.g. as low as 803 K after 80 h of air oxidation (4). The scales consist of a mixture of NiO and Nb oxides mainly $Nb_2O_5$, and some $NbO_2$. NbO was not found. The double oxide $NiNb_2O_6$ may form more internally similarly to crystalline Ni–Nb alloys oxidized at these temperatures [7].

Cross-sectional X-ray mapping revealed that the scale that builds up during the air oxidation consists, in general, of an outer layer of Ni oxide and a continuous inner layer of Nb oxide. This sequence of different oxide layers is repeated as the oxidation process proceeds. Fig. 7 shows one of these analyses on an oxidized sample at 833 K for 8 h. In this figure the multilayered scale it is visible in the Nb- and Ni-map. Sn is homogeneously dispersed as shown in the Sn-map. In addition the depletion of Nb in the alloy matrix underneath the scale is noticeable in the scattering electron photomicrograph as well as in the Nb- and Ni-map. This depletion in Nb may be the cause of the induced crystal-

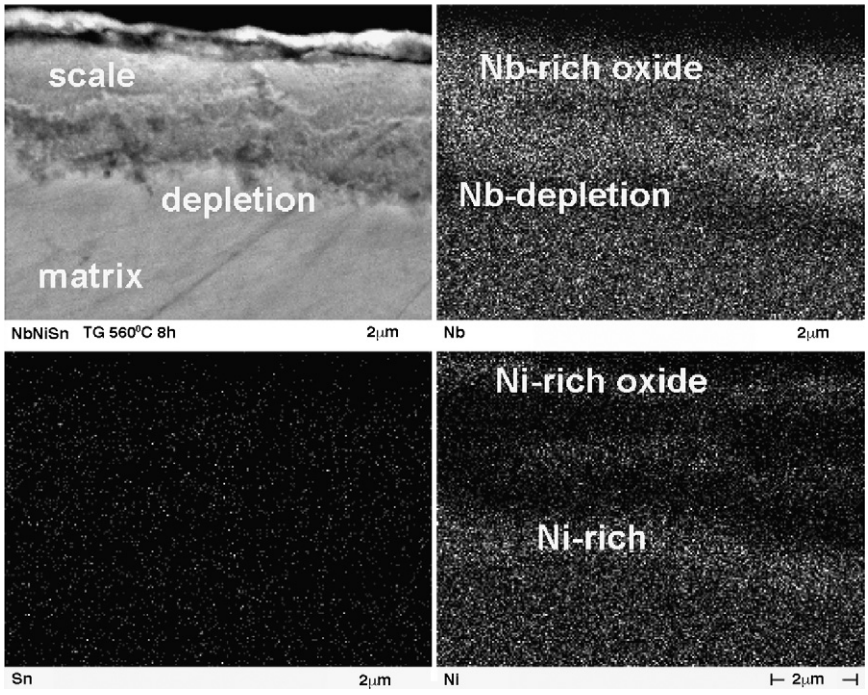


Fig. 7. Cross-sectional X-ray mapping at 10 kV of an oxidized samples at 833 K for 8 h.

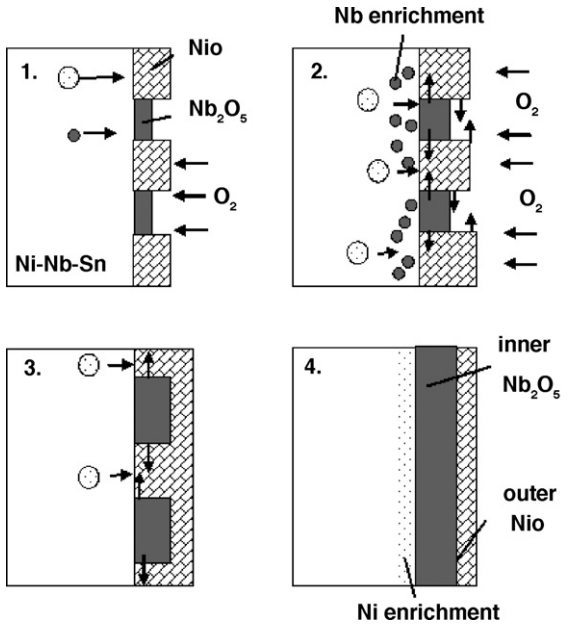


Fig. 8. Schematic illustration of the microstructure resulting from the oxidation of Nb–Ni–Sn glasses.

lization of the Ni-rich intermetallics that have been detected by X-ray diffraction.

The mechanism for the air oxidation of the RAG $Nb_{35}Ni_{60}Sn_5$ may be compared to that on a binary Nb–Ni involving the following steps, which are also schematically drawn in Fig. 8: (1) NiO and $Nb_2O_5$ nucleate at the surface; (2) $Ni^{2+}$-diffusion in NiO is faster than $Nb^{+}$-diffusion in $Nb_2O_5$ inducing lateral overgrowth of NiO; (3) Nb reduces NiO at their common interface: $2Nb + 5NiO \rightarrow Nb_2O_5 + 5Ni$; (4) the growth rates of the scales can be correlated to the diffusivities of O in fine-grained NiO and $Nb_2O_5$.

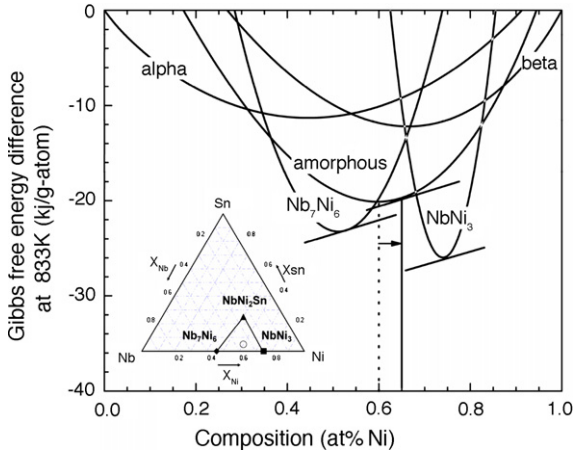


Fig. 9. Gibbs free energy diagram for the binary Nb–Ni calculated at 833 K after Bormann and Busch [5]. The Nb–60 at% Ni composition is marked with a dotted line. From the double tangent construction, a Ni-enrichment (Nb depletion) would cause an increase in driving force for the formation of $NbNi_3$ in the binary, and of $NbNi_3$ and $NbNi_2Sn$ in the ternary (see the ternary isothermal section in the inlet). The driving force for the formation of $Nb_7Ni_6$ decreases with increasing Nb depletion up to a point at which $Nb_7Ni_6$ cannot thermodynamically form.

Further experiments of the initial state of the oxidation (step 1), such as selecting shorter oxidation times, are necessary to confirm this mechanism. It has been to noted that in amorphous sputter deposited $Ni_{60}Nb_{40}$ [8] and $Ni_{65}Nb_{35}$ [9] oxidized in $O_2$ at low temperatures (room to 773 K) the surface is primarily $Nb_2O_5$ while a NiO layer has been found to form on top of the $Nb_2O_5$ layer after longer exposures.

The matrix gets enriched in Ni underneath the growing Nb oxide (step 3). This may induce crystallization of Ni-rich intermetallics by destabilizing the amorphous phase. Fig. 9 shows a Gibbs free energy diagram for the binary Nb–Ni calculated at 833 K after Bormann and Busch [10]. According to the double tangent construction of Fig. 9, the Ni-enrichment (Nb depletion) of the glassy matrix underneath the oxide scale is causing a destabilization of the amorphous phase and an increase in driving force for the formation of $NbNi_3$ in the binary, and of $NbNi_3$ and $NbNi_2Sn$ in the ternary (see the ternary isothermal section in the inset of Fig. 9). The driving force for the formation of $Nb_7Ni_6$ decreases with increasing Nb depletion up to a point at which $Nb_7Ni_6$ cannot thermodynamically form.

## 4. Conclusion

The $Nb_{35}Ni_{60}Sn_5$ refractory alloy glass shows good oxidation resistance at high temperatures up to 863 K. Isothermal thermogravimetric analyses revealed paralinear oxidation kinetics with similar oxidation rates that Zr-based glasses experience 200 K below. X-ray diffraction and cross-sectional electron microscopy allowed phase identification in the scales and revealed the oxide formation mechanism. The oxide scale consists of an outer layer of Ni oxide and a continuous inner layer of Nb oxide. This sequence of different oxide layers is repeated as the oxidation process proceeds. The depletion of Nb in the alloy underneath the scale may induce the crystallization of Ni-rich intermetallics such as $NbNi_3$ and $NbNi_2Sn$ as supported by thermodynamics concepts.

## Acknowledgements

The authors thank Monika Meuris (University of Dortmund) for the SEM and TEM studies. This material is based upon work supported by the National Science Foundation under the Grant no. DMR-0205940.

## References

[1] H. Choi-Yim, D.H. Xu, W.L. Johnson, Appl. Phys. Lett. 82 (7) (2003) 1030–1032.
[2] U. Köster, Triwikantoro, Mater. Sci. Forum 360–362 (2001) 29–36.
[3] X.M. Wang, I. Yoshii, A. Inoue, Y.H. Kim, I.B. Kim, Mater. Trans. JIM 40 (1999) 1130–1136.
[4] S. Yi, J.K. Lee, W.T. Kim, D.H. Kim, J. Non-Cryst. Solids 291 (2001) 132–136.
[5] T. Zhang, A. Inoue, Mater. Trans. 43 (2002) 708–711.
[6] L. Shadowspeaker, R. Busch, Appl. Phys. Lett. 85 (2004) 2508–2510.
[7] Y. Niu, F. Gesmundo, F. Viani, F.C. Rizzo, J.F. Oliveira, Corr. Sci. 37 (1995) 2043–2058.
[8] T.M. Christensen, J. Vac. Sci. Technol. A 6 (3) (1988) 914–917.
[9] Z. Song, D. Tan, F. He, X. Bao, Appl. Surf. Sci. 137 (1999) 142–149.
[10] R. Bormann, R. Busch, J. Non-Cryst. Solids 117–118 (1990) 539–542.